EVALUATION OF CREEP CRACK GROWTH RATE IN TERMS OF CREEP FRACTURE MECHANISM FOR 316 STAINLESS STEEL

M. TABUCHI, K. KUBO and K. YAGI
National Research Institute for Metals
1-2-1 Sengen, Tsukuba, 305 Japan

ABSTRACT

The relationship between creep crack growth rate and fracture mechanism was investigated on 316 stainless steel. Very long-term creep crack growth tests were conducted. Three kinds of creep fracture mechanisms, i.e., wedge-type intergranular fracture, transgranular fracture and cavity-type intergranular fracture, were observed depending on testing conditions. Creep crack growth rate was the fastest for wedge-type fracture mechanism and secondary for cavity-type and the slowest for transgranular fracture. The difference of crack growth rate was interpreted due to the creep rupture ductility corresponding to each creep fracture mechanism, except cavity-type fracture mechanism. Under the cavity-type fracture condition, crack growth rate increased as the creep damaged zone ahead of the crack tip increased.

KEYWORDS

Creep crack growth, 316 stainless steel, Creep fracture mechanism, C^* parameter, Long-term creep crack growth tests, Rupture ductility, Creep damaged zone

INTRODUCTION

It is important to predict the creep crack growth rate for the reliability evaluation of high temperature structural components. Creep fracture mechanism changes dependent on temperatures and stresses. In the long-term services, creep crack growth by grain boundary cavitation would be important. It is necessary to clarify the creep crack growth behaviour connecting with microscopical fracture mechanism for developing more accurate life prediction method. Although there are many engineering fracture mechanical studies on creep crack growth (Landes *et al.*, 1976, Harper *et al.*, 1977, Koterazawa *et al.*, 1977, Ohji *et al.*, 1977, and Taira *et al.*, 1979), experimental studies from the viewpoint of microscopical fracture mechanism are scarcely conducted(Ohtani *et al.*, 1991, Tabuchi *et al.*, 1992).

In the present work, creep crack growth tests including over 10,000h tests were conducted using CT specimen of 316 stainless steel. Three kinds of creep fracture mechanism were recognized in the creep tests for this material tested. The loading condition of the creep crack growth tests was chosen based on this creep fracture mechanism map. The relationship between creep crack growth behaviour and microscopical creep fracture mechanism was investigated.

EXPERIMENTAL PROCEDURES

Material and Specimen

The material tested is 316 stainless steel plate of 24mm in thickness. Chemical composition of this material is given in Table 1. The solid solution treatment condition was 0.5h at 1373K. The average grain size was about 50μm. The specimen used for the creep crack growth tests was CT specimen of 50.8mm in width and 12.7mm in thickness. Pre-crack of 2.5mm was introduced by fatigue loading at room temperature. After fatigue pre-cracking, sidegrooves of 20% of thickness were machined.

Table 1 Chemical composition of 316 stainless steel (mass%)

C	Si	Mn	P	S	Cu	Cr	Ni	Mo	Ti	Nb+Ta	B	Al	N
0.05	0.70	1.10	0.034	0.003	0.31	17.05	12.60	2.24	0.03	0.001	0.003	<0.003	0.017

Creep Crack Growth Test Procedure

Creep crack growth testing system is shown elsewhere (Tabuchi *et al.*, 1990). Creep crack length was measured by using D.C. electrical potential technique. Crack length was computed from the output voltage according to the Johnson's equation (Johnson, 1965). Load line displacement between upper and lower clevises which connect the specimen with pull rods was measured using extensometer and linear gauges. The creep crack growth tests were conducted at temperature range from 823K to 1073K. Long-term tests over 10,000h were conducted at 923K and 1023K.

Creep crack growth rate for ductile materials is generally evaluated by the non-linear fracture mechanical C^* parameter. In this study, the C^* parameter was calculated as follows (Ernst, 1983);

$$C^* = \frac{n}{n+1}\frac{P\dot{\delta}}{B_N(W-a)}\left(\gamma - \frac{\beta}{n}\right) \qquad (1)$$

where, B_N is the net thickness between the roots of sidegroove (=10.2mm), W is the specimen width (=50.8mm), a is the crack length, P is the load, $\dot{\delta}$ is the load line displacement rate, n is the creep exponent of Norton's rule and γ and β are the function of a and W. The value of n was obtained from the relationship between minimum creep rate *vs.* applied stress obtained from creep tests.

RESULTS AND DISCUSSION

Creep Fracture Mechanisms

The stress *vs.* time to rupture curves and the regions of three kinds of creep fracture mechanisms of round bar specimens were shown in Fig.1. In order to compare the fracture mechanisms of CT specimens with those of round bar specimens, the relation between gross section stress σ_g vs. time to rupture of CT specimens were also plotted. The gross section stress was calculated by the following equation (Landes *et al*, 1976) ;

$$\sigma_g = \frac{P}{\sqrt{BB_N}(W-a_0)}\left(1+3\frac{W+a_0}{W-a_0}\right) \qquad (2)$$

where, B is the specimen thickness(=12.7mm), a_0 is the initial crack length(=27.5mm).The region of creep fracture mechanisms shown in Fig.1 was determined according to the observation of fracture surface and microstructure. For higher stresses at lower temperatures, intergranular fracture due to the wedge-type cracking (W-type) was observed. For lower stresses at higher temperatures, intergranular fracture due to the growth of cavities formed at the interface between matrix and $M_{23}C_6$ or sigma phase precipitated on grain boundaries (C-type) was observed. Transgranular fracture (T-type) was observed between the conditions of W-type and C-type. Although the boundary between T-type region and C-type region of CT specimens is a little different from that of round bar specimens, the dependence of creep fracture mechanisms on testing conditions for CT specimens has the similar trend with those of round bar specimens.

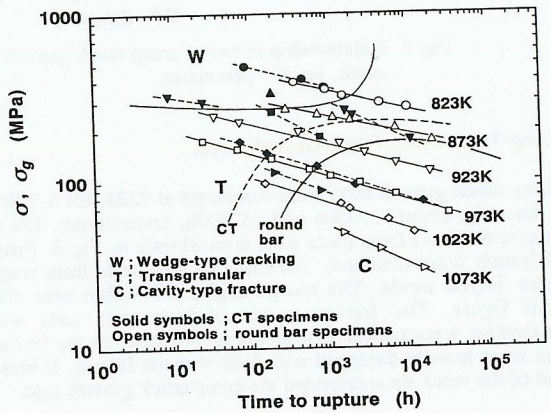

Fig.1 Relationship between stress *vs.* time to rupture, and creep fracture mechanisms of round bar specimens and CT specimens.

Relationship between Creep Crack Growth Rate and Fracture Mode

The relationship between creep crack growth rate, *da/dt*, and C^* parameter obtained under relevant creep fracture mechanism condition is shown in Fig.2. Because the crack growth rate at initial transient stage could not be evaluated by C^*(Yokobori *et al.*, 1988), those plots of initial stage were omitted in this figure. The *da/dt vs.* C^* relations depend on the microscopic creep crack growth mechanism. The creep crack growth rate under testing condition corresponding to W-type mechanism was the fastest, that under T-type was the slowest, and that under C-type was medium. The creep crack growth rate for C-type creep fracture mechanism was scattered between the upper bound for W-type and the lower bound for T-type. The creep fracture mechanism happened in engineering components would be C-type. Therefore, the creep crack growth tests under the testing condition corresponding to C-type would be more important and longer time test would be important.

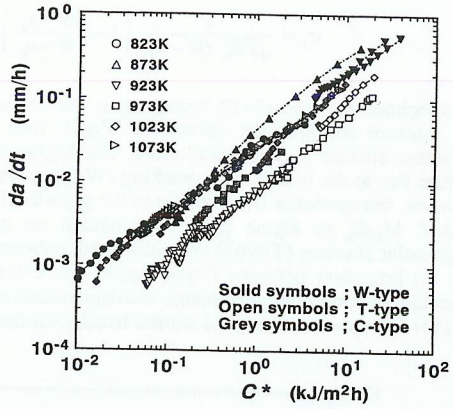

Fig.2 Relationship between creep crack growth rate, *da/dt*, *vs.* C^* parameter.

Results of Long-Term Creep Crack Growth Tests

Long term creep crack growth tests were conducted at 923K for 5.22kN and 1023K for 1.88kN. The rupture time was about 11,000h and 15,000h, respectively. The relationship between *da/dt vs.* C^* parameter obtained from these tests were shown in Fig.3. From these tests, the data that *da/dt* was 10^{-4}mm/h were obtained. The *da/dt* of long term tests was faster than that of short-term test under T-type mode. The morphologies of section near fractured surface were also shown in this figure. The fracture mode of long term tests was cavity-type and many intergranular cavities were observed near the main crack. In the test at 1023K for 1.88kN, the specimen was most heavily damaged and *da/dt* was the fastest. It was considered that the creep damage ahead of the crack tip accelerated the creep crack growth rate.

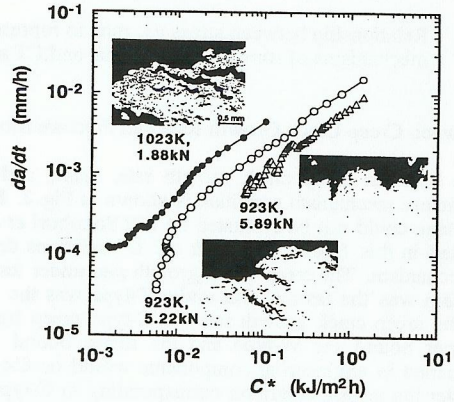

Fig.3 Relationship between *da/dt vs.* C^* parameter obtained from long-term tests more than 10000 hours.

Evaluation of Creep Crack Growth Rate Using Creep Ductility

The difference of creep ductility between fracture modes is considered to be one of the reason why *da/dt* depends on creep fracture mode. The relationship between *da/dt* and C^* parameter depends on the creep rupture ductility of testing materials (Nikbin *et al.*, 1986). Fig.4 shows the reduction of area *vs.* time to rupture relations in creep tests of round bar specimens. The reduction of area was dependent on creep fracture mechanism, and that is low for W-type creep fracture mechanism, high for T-type, and medium for C-type.

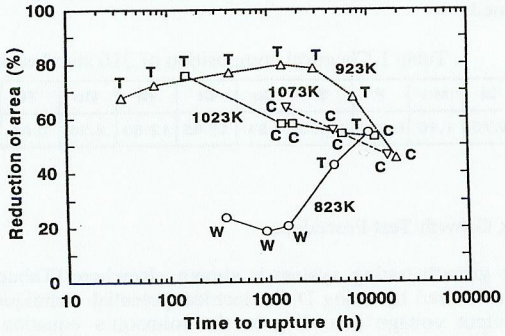

Fig.4 Relationship between reduction of area *vs.* time to rupture in creep tests of round bar specimen.

Fig.5 shows the relationship between creep crack growth rate at $C^* = 1$ kJ/m²h and reduction of area. The value of reduction of area in each creep crack growth test was estimated from the relationship between reduction of area and time to rupture in Fig.4. The relation of Fig.5 was dependent on creep fracture mechanisms. For the creep fracture mechanism conditions of W-type and T-type, the *da/dt* at $C^* = 1$ kJ/m²h was in inverse proportion to reduction of area as shown

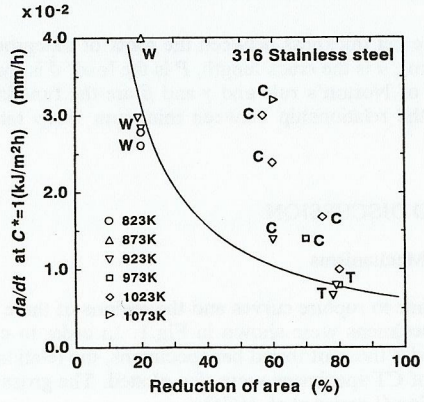

Fig. 5 Relationship between *da/dt* at C^* 1kJ/m²h *vs.* reduction of area.

with the solid curve in Fig.5. Creep crack growth rate for W-type and T-type could be written as follows;

$$\frac{da}{dt} = \frac{6.26\times10^{-3}}{\varepsilon_f^*} C^{*0.92} \qquad (3)$$

where, ε_f^* is the creep rupture ductility.

For C-type fracture mode, however, *da/dt* was faster than that predicted from equation(3). As mentioned above, the *da/dt* for C-type became faster as the temperature increased or time increased. When no crack is formed ahead of the main crack tip, i.e., under the condition of W-type and T-type creep fracture mechanisms, the creep crack growth rate depends on the creep rupture ductility. On the other hand, when many cracks and cavities are formed ahead of crack tip, the creep crack growth rate is faster than that estimated by the relation in which the creep rupture ductility is taken into account. In order to predict the creep crack growth rate under creep fracture mechanism condition of C-type, it is necessary to consider not only creep ductility but the effect of creep damage ahead of the main crack tip.

Creep Crack Growth Modeling by Grain Boundary Cavitation

It was considered that creep damage ahead of the main crack affect the macroscopic crack growth rate. Creep crack growth rate by cavitation was given as follows(Riedel, 1986).

$$\frac{da}{dt} = \frac{\pi(\tilde{\sigma}_e)^n (A\lambda)^{1/n+1}}{0.4(\lambda/d)(\tilde{\sigma}_e/\tilde{\sigma}_1)\sin(\pi\alpha)} \cdot \left(\frac{C^*}{I_n}\right)^{\alpha} \cdot \left\{\left(\frac{a-a_0}{\lambda}\right)^{1/n+1} - \frac{\Gamma(\alpha)}{\Gamma(2-\alpha)\Gamma(2\alpha-1)}\right\} \qquad (4)$$

where, $\alpha=n/n+1$, λ is the cavity spacing, d is the length of grain facet, I_n is the function of n and $\tilde{\sigma}_e$, $\tilde{\sigma}_1$ is the normalized equivalent stress and maximum principal stress. According to equation(4), *da/dt vs. C** relation depends on the crack length at the initial stage of crack growth. However, this effect can be negligible, when we discuss the crack growth rate at the steady state and accelerating stage. The comparison of experimental results at 1023K with equation(4) was

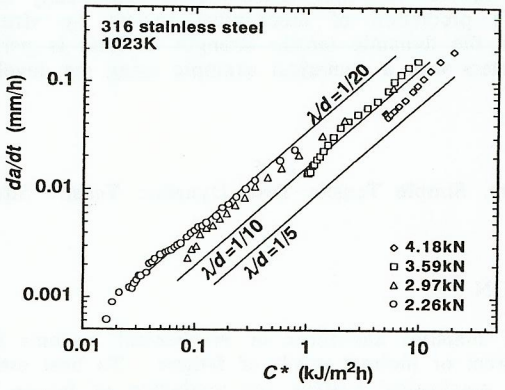

Fig.6 Comparison of creep crack growth model by grain boundary cavitation with experimental results.

shown in Fig.6. When we assume that the number of cavities on one grain facet is from 10 to 20, experimental results coincide well with the result obtained from theoretical equation.

Fig.7 shows the observed cavities ahead of the main creep crack. It is difficult to compare the observed cavity spacing with estimated one because the damage distribution is not constant. However, the experimental result that creep damage accelerate the crack growth rate is explained using this model.

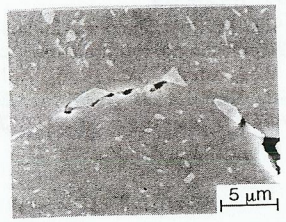

Fig.7 Grain boundary cavities observed ahead of the crack tip.

CONCLUSIONS

Creep crack growth tests were carried out using CT specimens on 316 stainless steel, and the effect of creep fracture mechanism on creep crack growth behaviour was investigated. The results are summarized as follows:

(1) Three types of creep fracture mechanisms, i.e., wedge-type cracking, transgranular fracture and cavity-type fracture, were observed on 316 stainless steel.

(2) Creep crack growth rate was evaluated by C^* parameter. Creep crack growth rate was dependent on microscopic creep fracture mechanism. The *da/dt* was the fastest for W-type fracture mechanism and the lowest for T-type.

(3) The difference of *da/dt* between W-type and T-type could be characterized by the creep rupture ductility.

(4) The creep cavities formed ahead of the crack were considered to affect the crack growth rate. Creep crack growth rate under cavity-type fracture mechanism should be predicted by considering not only creep ductility but the creep damage density.

REFERENCES

1. Landes, J.D. and Begley, J.A. (1976). A fracture mechanics approach to creep crack growth. *Mech. of Crack Growth, ASTM STP 590*, 128-148.
2. Harper, M.P. and Ellison, E.G. (1977). The use of the C^* parameter in predicting creep crack propagation rates. *J. Strain Analysis*, **12**, 167-179.
3. Koterazawa, R. and Mori, T. (1977). Applicability of fracture mechanics parameters to crack propagation under creep condition. *J. Soc. Mat. Sci. Jpn.*, **26**, 948-954.
4. Ohji, K., Ogura, K. and Kubo, S. (1978). *Trans. Jpn. Soc. Mech. Eng.*, **44**, 1831-1837.
5. Taira, S., Ohtani R. and Kitamura, T. (1979). Application of *J*-integral to high-temperature crack propagation.*Trans. ASME, J. Eng. Mat. Tech.*, **101**, 154-161.
6. Ohtani, R., Kitamura, T. and Zhow, W. (1991). Effect of compressive creep on crack propagation of type 304 stainless steel under time-dependent creep-fatigue conditions. *J. Soc. Mat. Sci. Jpn.*, **40**, 1290-1296.

7. Tabuchi, M., Yagi, K. and Ohba, T. (1990). Characterization of creep crack growth behaviour of 316 stainless steel in terms of microscopical fracture mechanism. *ISIJ International*, **30**, 847-853.
8. Tabuchi, M., Kubo, K. and Yagi, K. (1992). Long-term creep crack growth behaviour of 316 stainless steel. *J. Soc. Mat. Sci. Jpn.*, **41**, 1255-1260.
9. Johnson, H.H. (1965). Calibrating the electric potential method for studying slow crack growth. *Materials Research and Standards*, **5**, 442-445.
10. Ernst, H.A. (1983). Unified Solution for J ranging continuously from pure bending to pure tension. *ASTM STP 791*, I-499-519.
11. Yokobori, A.T. and Yokobori, T. (1988). The crack initiation and growth under high temperature creep, fatigue and creep-fatigue multiplication. *Eng. Frac. Mech.*, **31**, 931-945.
12. Nikbin, K.M., Smith, D.J. and Webster, G.A. (1986), An engineering approach to the prediction of creep crack growth. *Trans. ASME, J. Eng. Mater. Tech.*, **108**, 186-191.
13. Riedel, H. (1986). *Fractur at High Temperatures, Chap 21*, pp.272-285. Springer-Verlag, Berlin